Energy management of cooperative microgrids: A distributed optimization approach

Tian Liu[a],*, Xiaoqi Tan[a], Bo Sun[a], Yuan Wu[b], Danny H.K. Tsang[a]

[a] Department of Electronic and Computer Engineering, Hong Kong University of Science and Technology, Hong Kong
[b] College of Information Engineering, Zhejiang University of Technology, Hangzhou 310023, China

A B S T R A C T

The cooperation of multiple networked microgrids (MGs) can alleviate the mismatch problem between distributed generation and demand and reduce the overall cost of the power system. Energy management with direct energy exchange among MGs is a promising approach for improving energy efficiency. However, existing methods on microgrid cooperation usually overlook the underlying distribution network with operating constraints (e.g., voltage tolerance and power flow constraints). Hence the results may not be applicable to actual systems. This paper studies the energy management problem of multiple MGs that are interconnected by both the direct current (DC) energy exchange network and the alternating current (AC) traditional distribution networks. In our problem, each MG is equipped with renewable energy generators as well as distributed storage devices. In order to handle the non-convex power flow constraints, we exploit the recent results of the exact optimal power flow (OPF) relaxation method which can equivalently transform the original non-convex problem into a second-order cone programming problem and efficiently determine the optimal solution successfully. The objective of our problem is to minimize the overall energy cost in a distribution network consisting of multiple MGs, with the practical operating constraints (e.g., power balance and the battery's operational constraints) explicitly incorporated. Considering the privacy and scalability, we propose a distributed algorithm with convergence assurance based on the alternating direction method of multipliers (ADMM). We also implement our method based on the model predictive control (MPC) approach in order to handle the forecasting errors of the renewable energy generation. Simulations are made for different MG exchange topologies on three radial distribution network testbeds. Numerical results demonstrate that certain topologies are more favorable than others, and the cooperation strategy for the energy exchange is significantly affected by the MGs' locations in the distribution network.

1. Introduction

1.1. Motivation and Methodology

Microgrids (MGs) are localized grids which accommodate a variety of distributed energy resources (DERs) and different types of energy users. They are believed to be a promising paradigm that can improve the utilization of DERs and also users' benefits [1]. However, in order to ensure the stability and reliability of MGs, many tough problems need to be resolved, among which, the mismatch between the distributed generations and loads due to the intermittent nature of DERs (e.g., photovoltaic (PV) generators and wind turbines (WT)) is a key issue and draws lots of attention. In order to handle this, several approaches can be employed.

One solution is to take advantage of distributed storage (DS) devices

(e.g., batteries), which however suffer from two drawbacks: a huge capital investment increases dramatically with DS capacities, and significant energy transfer loss occurs due to the inefficiency of charging and discharging processes. Therefore, relying solely on DS units is not enough. Another promising solution is the direct energy exchange among neighboring and cooperative MGs by dedicated energy exchange network (denoted as EEN hereinafter). An EEN is composed of direct power lines connecting a cluster of geographically correlated MGs, enabling energy sharing and trading among them [2]. By exploiting the diversified distributed generation and consumption profiles, EENs have the following advantages: first, reduced power transmission loss thanks to the short distance between MGs, and second, lower energy bills for the MGs because the internal energy trading price is higher than the buyback price, while lower than the selling price of the utility company [3,4]. Thanks to these advantages, MGs will have enough incentives to

Nomenclature

Abbreviations

$(\cdot)^l$, $(\cdot)^c$	local, consensus variables
cp, np	coupling, non-coupling variables
AC	alternative current
ADMM	alternating direction method of multipliers
DC	direct current
DER	distributed energy resource
DS	distributed storage
EEN	energy exchange network
LAO	local are operator
MG	microgrid
MPC	model predictive control
OPF	optimal power flow
PCC	point of common coupling
PV	photovoltaic
TOU	time-of-use
WT	wind turbines

Functions

$C_{n,t}^{ES}(\cdot)$	battery's operational cost
$C_t(\cdot)$	battery's operational cost
$C_t^P(\cdot)$	total energy purchase cost

Index

i	index of bus (node)
i_0	index of parent bus of i
i_n	bus index of MGs in distribution networks
k	index of iteration
m, n	index of MGs
t	index of time

Parameters

Ω_n^c, Ω_n^l	constraint sets for consensus and local variables for MGs
Ω_{lao}^c, Ω_{lao}^l	constraint sets for consensus and local variables for LAO
Δ	duration of a time slot

η_c, η_d	charging and discharging efficiencies
$\mathscr{E}$	branch set
$\mathscr{K}$	node set
$\mathscr{M}$	set of MGs
$\mathscr{N}$	index set of MGs
$\mathscr{T}$	tree representation of distribution networks
$\mathscr{W}$	index set of MGs in distribution networks
ω	weighting factors
$\overline{\gamma_n}$, $\underline{\gamma_n}$	upper and lower bounds for storage level at the end of the time horizon
$\overline{ES_n}$, $\underline{ES_n}$	upper and lower bounds of energy storage
$\overline{P_{n,t}^{ESC}}$, $\overline{P_{n,t}^{ESD}}$	charging and discharging power limits
$\overline{P_{n,t}^{inj}}$	power injection limits
$\overline{v_{i,t}}$, $\underline{v_{i,t}}$	upper and lower bounds of squared magnitude of bus voltage
H	total number of time slots
N	number of microgrids
N_i	set of the children buses
$P_{n,t}^{RE}$	renewable energy generation
PR_t	TOU price
$r_{m,n}$	line resistance between MG_m and MG_n
$S_{i,t}^L$, $P_{i,t}^L$, $Q_{i,t}^L$	apparent, active and reactive loads
$U_{m,n}$	sending end transmission voltage between MG_m and MG_n
z_i, r_i, x_i	impedance, resistance and reactance of branch
K	number of branches

Variables

$X_t^{(\cdot)}$	vector of decision variables
$X_{cp,t}^{(\cdot)}$, $X_{np,t}^{(\cdot)}$	vector of coupling, non-coupling variables for LAO/MGs
$ES_{n,t}$	remaining energy in the battery
$I_{i,t}$	branch current
$l_{i,t}$	squared magnitude of branch current
$P_{n,t}^{ESC}$, $P_{n,t}^{ESD}$	charging and discharging power
$S_{i,t}^A$, $P_{i,t}^A$, $Q_{i,t}^A$	apparent, active and reactive power drawn from the distribution network
$S_{i,t}$, $P_{i,t}$, $Q_{i,t}$	apparent, active and reactive power flows
$T_{m,n,t}$	power transfer from MG_m to MG_n
$V_{i,t}$	complex bus voltage
$v_{i,t}$	squared magnitude of bus voltage

cooperate with each other in order to minimize the overall cost of the system [5] and benefit from the energy sharing via the EEN. In fact, the similar concept of the peer-to-peer direct current (DC) EEN among MGs has been proposed in [6,7], and this DC EEN is in parallel to the underlying AC distribution network. Accordingly, we add the structured relationship between these two networks in Fig. 1. From the figure, we can see that each MG is connected to the traditional AC distribution network and at the same time, they are interconnected by a dedicated DC EEN. The EEN enables the direct energy exchange among MGs and the connection to the distribution network can ensure the balance between supply and demand for each MG.

The coordinated energy management of networked MGs with energy sharing has been warmly discussed in the literature [8,5,9–15]. Gregoratti et al. [5] developed a distributed convex optimization framework for energy trading between islanded MGs, where all MGs cooperate with one another to minimize the total cost of the system. Lakshminarayana et al. [8] analyzed the tradeoff between the use of storage and the cooperation by energy sharing among DG resources with the objective of minimizing the time average cost of the energy exchange within the grid. A problem in these prior works is that the transmission loss incurred by the energy sharing is either ignored [8,5,9–11] or oversimplified by a linear model [12,13], both of which

are not realistic in practice. In contrast to these, some recent works considered the energy sharing problem of MGs with a more accurate loss model [14,15], by using a quadratic function of the energy transferred. Another issue in [8,5,9–15] is that their models were proposed in an abstract way with the underlying distribution networks neglected. In fact, the MGs, if not operated in an islanded mode such as those in remote areas, are connected with the main grid via the points of
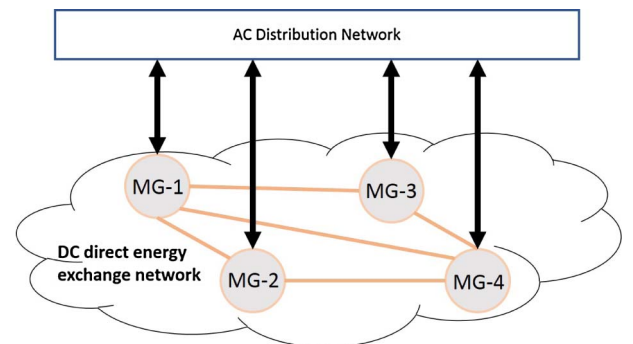

Fig. 1. DC direct energy exchange network of multiple MGs in parallel with the AC distribution network.

common coupling (PCC) through the distribution networks. For this reason, the associated power flow constraints and other system operational constraints [16–18] of the distribution networks should be taken into account such that the obtained scheme can be applicable to actual systems and truly benefits users with the stability [19] and reliability of the system ensured.

In this paper, motivated by the above considerations, we present a model for the energy management of cooperative MGs with energy sharing under distribution networks [20]. The context of our problem is the day-ahead market with a time-of-use (TOU) pricing mechanism. In our problem, there is a local area operator (LAO) in charge of constructing the EEN, for the purpose of reducing the system power loss and improving the energy efficiency. Moreover, the MGs are equipped with DERs (i.e., solar panels and wind turbines) and DS units (i.e., batteries). In this way, the MGs can fulfill their demands by not only their own distributed resources but also the supply from the EEN and the main grid. The objective of our problem is to minimize the overall system cost, which includes: (i) the money paid for the power fed into the network, (ii) the power loss in the distribution network, (iii) the direct energy exchange cost, and (iv) the battery's operational cost, while satisfying all the corresponding constraints, such as system operational constraints on power flow and voltage, and the batteries' operational constraints.

Our problem is formulated as a non-convex optimization problem since the resistive power losses in the distribution network are considered in an alternative current (AC) power flow model, and thus, an exact solution may be too complex to compute [5]. To handle the non-convex optimal power flow (OPF) problem more efficiently, in this paper we exploit the recent results of the exact OPF relaxation method from [21]. In particular, this method matches the property of our model well, thus enabling us to equivalently transform the original non-convex problem into a second-order cone programming problem and efficiently determine the optimal solution successfully (without suffering from any relaxation loss).

To solve the energy management problems of MGs, many centralized solutions have been used [9,10,12]. However, due to some disadvantages (e.g., poor scalability and privacy concerns) of the centralized solutions, distributed methods are more desirable [22]. For this reason, we develop a distributed algorithm to solve our problem based on the alternating direction method of multipliers (ADMM) [5,23] by leveraging the specific structure of our formulation, such that the MGs and LAO only need to communicate with their direct neighbors and hence the communication overhead can be quite low. Moreover, the convergence of the algorithm is assured.

We apply our model on three radial distribution systems (34-bus, 69-bus and 119-bus) and perform extensive numerical tests. Specifically, the fast convergence rate of our proposed algorithm is demonstrated with appropriate chosen parameters. Furthermore, the results show that different MGs can cooperate with each other according to their distinct and/or complementary consumption profiles to minimize the total cost of the system. In addition, simulations are conducted for different EEN topologies, which show that, depending on the relative positions of MGs in the distribution network, some specific EEN topologies may be more advantageous. Moreover, considering the uncertainty of the renewable energy input, we also implement our method based on the model predictive control (MPC) approach in order to handle the forecasting errors of the renewable energy generation. The results show that with estimation errors, performance loss of our method is still acceptable.

1.2. Related works

There are several works in the literature that have studied the interaction of multiple MGs with the distribution networks [17,24–29]. In [17,24], the authors propose a control strategy for the coordinated operation of networked microgrids (MGs) in a distribution system. They formulate the problem as a stochastic bi-level optimization problem in which the upper level problem is solved by the distribution operator in order to guarantee the operational constraints while the lower level problem is to minimize the operation costs of MGs. In [25–27], a bi-level optimal operation model for distribution networks with grid-connected MGs have been presented. The upper-level model determines the optimal dispatch of the distribution network to achieve its power loss reduction and voltage profile improvement, while the lower-level model determines the optimal operation strategy of distributed generators in MGs considering the utilization of renewable power. However, in [25], although the operation of multiple grid-connected MGs are considered, only the interaction between the distribution network and MGs is studied without considering any power exchange among MGs. By contrast, in [26,27], the cooperative interaction among MGs with expanded energy storage systems are taken into account in addition to the interaction with the distribution network. Specifically, the cooperation among MGs is modeled by an interactive energy game matrix based on priority-based game theory to take full advantage of the remaining dispatchable capacity in energy storage systems and distributed generators. In [26], the impact of the large integration of renewable energy resources is considered and analyzed. Moreover, the authors in [27] introduce the responsive reserve of distributed generators to the model to improve the system operation. Additionally, the authors in [28] propose an optimal energy scheduling framework for the energy exchange among multiple microgrids while considering the security constraints. In their framework, there are two layers: a distributed network layer which solves the OPF problem and a market layer which coordinates the energy transaction among multiple MGs. Furthermore, in [29], a distributed algorithm for the energy management of networked MGs based on the on-line alternating direction method of multipliers algorithm is proposed. Their objective is to coordinate the power scheduling of various components in the MGs while satisfying the underlying power network operation constraints.

Compared with our work, there are several issues in these related works. The most remarkable one is that although the problems in those literature have considered networked MGs with a distribution system, there is no direct energy exchange network among MGs. Specifically, they only allow the MGs to exchange energy through the distribution network. In contrast, in our work both the DC EEN as well as the interaction between the MGs and the distribution network are taken into account. Therefore, the energy management for the coordination between the EEN and the traditional distribution networks is studied in our work, which is one of our key contributions. In addition, although the similar concept of the peer-to-peer DC energy exchange network among MGs has been proposed in [6,7], the detailed energy management problem involving these two networks has not been studied. Hence, our work tries to make the first attempt to fill this gap in the literature.

Furthermore, the problem formulation in our work is more practical in several aspects when compared to those works in the literature. For example, in [17,24,29], linearized power flow equations for distribution networks are used, while in our work, an AC power flow model has been adopted which is more accurate. Moreover, in [17,24,28,29], the DS devices are not considered, while our model involves DS devices because they are becoming more and more important with the increasing penetration of renewable energy resources.

In addition, although in [24,28], distributed algorithms are proposed for the energy management of networked MGs, there is no theoretical proof of the convergence. The lack of the convergence guarantee may raise concern about the reliability of their methods. In [29], an on-line ADMM algorithm is leveraged for solving their problem. Compared to their work, one important contribution of our work is that we have proved that the primal decision variables converge to the optimal values. This is stronger than a general convergence result of the ADMM algorithm applied to a convex problem where only the objective value are guaranteed to converge to the optimal value.

1.3. Contributions

We summarize the main contributions of our work as follows.

1. The energy management for multiple MGs that are interconnected by both the DC EEN and the AC distribution network has been studied. In our problem, the distributed storage devices are taken into account such that the energy can be stored and released in order to help complement the instant energy deficiency or surplus at different time of the day. Moreover, the AC power flow equations without any approximation are used to accurately model the power flow and operational constraints of the distribution networks.

2. We propose a distributed approach such that the disadvantages of centralized methods (e.g., poor scalability, privacy concerns and high communication overhead) can be avoided with the assurance of convergence of our proposed algorithm. Another advantageous feature of our ADMM-based algorithm is that we prove that the primal decision variables converge to the optimal values, which is stronger than a general convergence result of the ADMM algorithm.

1.4. Organization

The rest of the paper is organized as follows. In Section 2, the MG EEN and the distribution network are modeled. The problem formulation as well as its relaxed version is discussed in Section 3. The distributed algorithm is described in Section 4. Numerical results are presented in Section 5, followed by conclusions in Section 6.

2. System model

2.1. MG direct energy exchange network model

We consider a set of N MGs, denoted by $\mathscr{M} = \{MG_n : n \in \mathscr{N}\}$, where $\mathscr{N} = \{1, \ldots, N\}$, and $\mathscr{W} = \{i_n : n \in \mathscr{N}\}$ denotes the corresponding index set of MGs, where i_n denotes the index of MG_n in the distribution network. The time horizon is discretized, and $t \in \{1, 2, \ldots, H\}$ denotes the time slot $(t, t + \Delta]$, where H is the total number of time slots of interest. Each MG is connected to a bus of the underlying distribution network by the PCC, and is equipped with a battery as well as DERs (PV generators and WTs). These MGs are also connected by an EEN. Note that this EEN network is a direct current (DC) network, through which only active power is shared among MGs. Fig. 2 is an example of a three-MG EEN. At each time slot t, if MG_m transfers $T_{m,n,t}$ amount of active power to MG_n, then the power received by MG_n is [14,15]

$$T_{m,n,t} - \frac{r_{m,n} T_{m,n,t}^2}{U_{m,n}^2} \quad \forall \ t, m, n, m \neq n, \tag{1}$$

where $r_{m,n}$ denotes the resistance of the transmission line and $U_{m,n}$ denotes the transmission voltage, which is the sending end voltage of the line (m, n).

This model is applicable to any energy exchange topology since it focuses on the power transferred on each line in an arbitrary topology. More specifically, as in Fig. 1, if $T_{1,3,t}$ is 15 kW and $T_{3,2,t}$ is 10 kW, it means that at time slot t, 10 kW of the power is transferred from MG_1 to MG_2 passing through MG_3, while 5 kW is supplied to MG_3. Obviously, MG_1 can also transfer power through the direct line to MG_2. So our model can cover all the possible paths between any two MGs. Note that $T_{m,n,t}$ is different from $T_{n,m,t}$, and each represents power transference, but in opposite directions. Therefore, they are non-negative and should not be nonzero simultaneously:

$$T_{m,n,t} \geqslant 0, \quad \forall \quad m, n, t, \tag{2}$$

$$T_{m,n,t} \cdot T_{n,m,t} = 0, \quad \forall \quad m, n, t. \tag{3}$$

2.2. DS device model

We use $ES_{n,t}$ to denote the remaining energy level in the battery of MG_n at time slot t, and it evolves as follows:

$$ES_{n,t+1} = ES_{n,t} + \left(\eta_c P_{n,t}^{ESC} - \frac{1}{\eta_d} P_{n,t}^{ESD}\right)\Delta, \quad \forall \ n, t, \tag{4}$$

where $P_{n,t}^{ESC}$ (or $P_{n,t}^{ESD}$) denotes the charging (or discharging) power, and $\eta_c, \eta_d \in (0,1]$ are the charging and discharging efficiencies, respectively. Note that the charging and discharging rates are respectively limited by the power ratings $\overline{P_{n,t}^{ESC}}$ and $\overline{P_{n,t}^{ESD}}$, and they cannot be nonzero at the same time. Also, the storage level should be within a certain range at each time slot and the constraints are given as follows:

$$0 \leqslant P_{n,t}^{ESC} \leqslant \overline{P_n^{ESC}} \quad \forall \ n, t, \tag{5}$$

$$0 \leqslant P_{n,t}^{ESD} \leqslant \overline{P_n^{ESD}} \quad \forall \ n, t, \tag{6}$$

$$P_{n,t}^{ESC} \cdot P_{n,t}^{ESD} = 0 \quad \forall \ n, t, \tag{7}$$

$$\underline{ES_n} \leqslant ES_{n,t} \leqslant \overline{ES_n} \quad \forall \ n, t, \tag{8}$$

where $\underline{ES_n}$ and $\overline{ES_n}$ denote the lower and upper bounds of the permitted storage levels, respectively. In addition, the battery's operational cost $C_{n,t}^{ES}$ is modeled by its conversion loss, i.e.,

$$C_{n,t}^{ES} = (1 - \eta_c) P_{n,t}^{ESC} + \left(\frac{1}{\eta_d} - 1\right) P_{n,t}^{ESD} \quad \forall \ n, t. \tag{9}$$

Moreover, we set a lower bound and an upper bound for the storage level at the end of the time horizon such that both charging and discharging will be available for the future:

$$\underline{\gamma_n} \cdot \overline{ES_n} \leqslant ES_{n,H} \leqslant \overline{\gamma_n} \cdot \overline{ES_n}, \tag{10}$$

where $0 \leqslant \underline{\gamma_n} \leqslant \overline{\gamma_n} \leqslant 1$.

Note that this paper focuses on the short-term energy scheduling of MGs, and thus, the battery lifetime and degradation cost are not considered. For detailed quantification analysis about the battery lifetime and degradation cost, please refer to our previous works [30,31].

2.3. Renewable energy generation and demand models

2.3.1. Renewable energy generation

Each MG is equipped with a PV generator and a WT. In our day-ahead scheduling problem, we use $P_{n,t}^{RE}$ to denote the renewable energy generation of MG_n at time slot t. First, we assume that $P_{n,t}^{RE}$ can be predicted for the next 24 h with tolerant errors and second, the prediction errors are handled by applying our method with an MPC-based approach (in Section 5). We emphasize that our problem mainly focuses
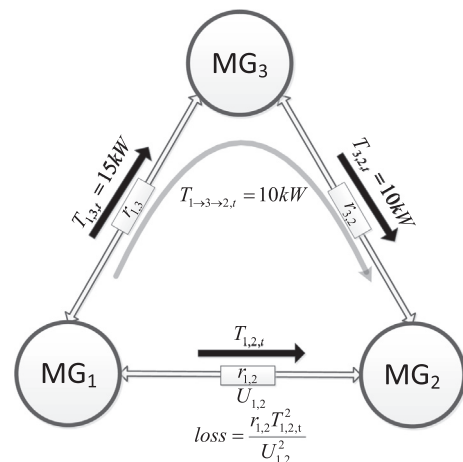

Fig. 2. An example of a three-MG EEN.

on understanding the tradeoff between energy storage, direct energy exchange of MGs and the interaction with the main grid in a day-ahead manner, thus the detailed prediction methods of the renewable energy generation is beyond the scope of this paper.

2.3.2. Demands

The load demands of MGs and other buses can have active and reactive parts, which are denoted by

$$S_{i,t}^L = P_{i,t}^L + jQ_{i,t}^L, \tag{11}$$

where i is the index of nodes in the distribution network. The demands of MGs can be met by either self renewable generation, battery discharging, energy exchange with other MGs or purchasing from the main grid.

2.4. Distribution network model

A distribution network in most cases is a radial network and can be represented by a tree $\mathscr{T} = (\mathscr{K}, \mathscr{E})$, where $\mathscr{K}$ and $\mathscr{E}$ denote the node set and the branch set, respectively. Each node (bus) indexed by $i \in \mathscr{K} = \{1,...,K\}$ is either a pure load or an MG, and $|\mathscr{E}| = K$ is the cardinality of the branch set. The tree is rooted at the substation bus indexed by $i = 1$. In a radial network, every node $i \in \mathscr{K} \backslash \{1\}$ has a unique parent bus denoted by i_0. Thus, we can simplify the notation index of variables on directed branches (i_0, i) to be i. In Fig. 3, for instance, at time slot t, the complex power flow from node i_0 to node i can be defined as

$$S_{i,t} = P_{i,t} + jQ_{i,t} = V_{i_0,t} I_{i,t}^*, \qquad \forall \ t, i \in \mathscr{K} \backslash \{1\}, \tag{12}$$

where $P_{i,t}$ and $Q_{i,t}$ are active and reactive parts of the power flow, respectively.

It should be noted that we only consider the single-phase balanced distribution systems. Moreover, only the overhead lines, instead of cables, are studied in the distribution network, such that the line capacitances are ignored. Extension of this work to taking into account the line capacitances as well as more devices such as shunt capacitors and transformers in unbalanced distribution networks can be an interesting future work.

We denote z_i, x_i and r_i as the branch impedance, reactance, and resistance, respectively, and we use $v_{i,t}$ and $l_{i,t}$ to denote the squared magnitude of the bus voltage $V_{i,t}$ and the branch current $I_{i,t}$, respectively. Therefore, based on the branch flow model [32], the relationship among these parameters can be summarized as follows, $\forall \ t, i \in \mathscr{K} \backslash \{1\}$,

$$P_{i,t}^A = P_{i,t} - r_{i,t} l_{i,t} - \sum_{k \in N_i} P_{k,t}, \tag{13}$$

$$Q_{i,t}^A = Q_{i,t} - x_{i,t} l_{i,t} - \sum_{k \in N_i} Q_{k,t}, \tag{14}$$

$$v_{i,t} = v_{i_0,t} + (r_i^2 + x_i^2) l_{i,t} - 2(r_i P_{i,t} + x_i Q_{i,t}), \tag{15}$$

$$l_{i,t} = \frac{P_{i,t}^2 + Q_{i,t}^2}{v_{i_0,t}}, \tag{16}$$

where $P_{i,t}^A$ and $Q_{i,t}^A$ denote the active and reactive power drawn out of the distribution network to the load at bus i, respectively. $N_i = \{j \in \mathscr{K}: j_0 = i\}$ is the set of the children buses of i. Eqs. (13) and (14) are the power conservation equations, where $r_{i,t} l_{i,t}$ represents the power loss on branch i. Eq. (15) comes from the combination of (12) and Ohm's law after some simple manipulation. Eq. (16) is from (12) after squaring. The voltage at each bus needs to be restricted in an allowable range to ensure the system stability and security:

$$\underline{v_i} \leqslant v_{i,t} \leqslant \overline{v_i} \qquad \forall \ t, i \in \mathscr{K} \backslash \{1\}, \tag{17}$$

where $\underline{v_i}$ and $\overline{v_i}$ are the lower and upper bounds of the squared magnitude of bus voltage, respectively. Note that at the root bus ($i = 1$), the

voltage is fixed as V_1 (i.e., $v_{1,t} \equiv v_1$) where V_1 is the rated voltage. Another boundary condition is as follows:

$$-S_{1,t}^A = -(P_{1,t}^A + jQ_{1,t}^A) = \sum_{i \in N_1} S_{i,t}, \qquad \forall \ t, \tag{18}$$

which represents the total power injected into the distribution network. The total energy purchase cost is defined as:

$$C_t^P = PR_t \cdot (-P_{1,t}^A) \qquad \forall \ t, \tag{19}$$

where PR_t is the TOU price given by the main grid. Note that $P_{1,t}^A$ is negative since at the substation ($i = 1$), power is *fed into* the distribution system.

We underline that our model has a two-level network structure, in which the EEN is isolated and separated from the distribution network and our energy sharing scheme only affects the amount of net power, $P_{i_n,t}^A$, injected (drawn) into (from) the distribution network. Therefore, the radial structure of the distribution network is not changed and the branch flow model is indeed applicable to our problem.

3. Problem formulation and exact relaxation

In this work, we consider the MGs which are willing to cooperate with each other to reduce the overall cost. These MGs have the sufficient incentive because the benefit of the overall cost reduction will be shared among the MGs such that each MG can pay a lower energy bill. The detailed mechanism for pricing and profit sharing in the EEN is beyond the scope of this paper, while our previous work about the pricing for hybrid energy trading market [3] is an example.

The objective of our problem is to minimize the total cost of the distribution network including: (i) the payoff for buying power from the main grid, (ii) the battery's operational cost, and (iii) the power loss costs in the distribution network and the EEN, with corresponding weighting factors $\omega_i, i \in \{1,...,4\}$. As for constraints, we take into account the mutual exclusive constraints on energy exchange powers (i.e., Eq. (3)), the power balance constraints (i.e., Eqs. (20)–(22)), the system operational constraints on the power flow (i.e., Eqs. (13)–(16)) and voltage (i.e., Eq. (17)) as well as the battery's operational constraints (i.e., Eqs. (4)–(8), (10)). Mathematically, the optimization problem is as follows: **Problem $\mathcal{P}$**

$$\min_{X_t} \quad \sum_{t=1}^H C_t(X_t)$$

$$\text{s.t.} \quad P_{i_n,t}^A + P_{n,t}^{RE} + \sum_{m \in \mathscr{N} \backslash \{n\}} \left(T_{m,n,t} - \frac{r_{m,n} T_{m,n,t}^2}{U_{m,n}^2} \right)$$

$$+ P_{n,t}^{ESD} \geqslant P_{n,t}^L + P_{n,t}^{ESC} + \sum_{m \in \mathscr{N} \backslash \{n\}} T_{n,m,t}, \tag{20}$$

$$Q_{i,t}^L \leqslant Q_{i,t}^A, \quad \forall \ t, i \in \mathscr{K} \backslash \{1\}, \tag{21}$$

$$P_{i,t}^L \leqslant P_{i,t}^A, \quad \forall \ t, i \in \mathscr{K} \backslash \mathscr{W}, \tag{22}$$

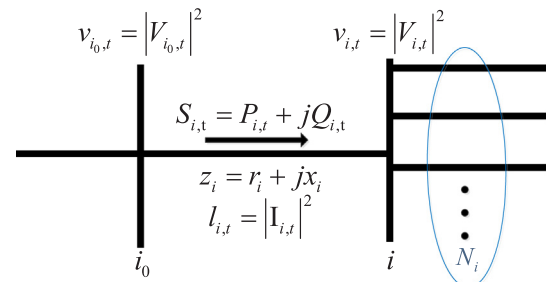$$-P_{i_n,t}^A \leqslant \overline{P_{n,t}^{inj}}, \quad \forall \ t, n \in \mathscr{N}, \tag{23}$$

Fig. 3. Branch flow model from bus i_0 to i.

(2)–(8), (10), (13)–(17),

where $X_t = (P_{i,t}^A, P_{n,t}^{ESC}, P_{n,t}^{ESD}, T_{m,n,t})$ is the vector of decision variables, and other state variables such as $P_{i,t}$, $Q_{i,t}$, $v_{i,t}$ and $l_{i,t}$ can be determined based on decision variables. In addition, the cost function $C_t(X_t)=$

$$\omega_1 PR_t(-P_{1,t}^A) + \omega_2 \sum_{i=2}^{K} r_i l_{i,t} + \omega_3 \sum_{n \in \mathcal{N}} \left[(1-\eta_c)P_{n,t}^{ESC} + \left(\frac{1}{\eta_d}-1 \right)P_{n,t}^{ESD} \right]$$
$$+ \omega_4 \sum_{n \in \mathcal{N}} \sum_{m \in \mathcal{N} \setminus \{n\}} \frac{r_{m,n} T_{m,n,t}^2}{U_{m,n}^2}.$$

$\mathcal{K} \setminus \mathcal{W}$ denotes the pure load bus set excluding MGs. Note that constraints (23) are imposed such that the power injection of MGs to the main grid is limited by the upper bounds $\overline{P_{n,t}^{inj}}$. In addition, the inequalities in Constraints Eqs. (20)–(22) actually allow the *over-satisfaction* of the loads. This kind of constraint has been used by many other papers [33–35]. The allowance for the over-satisfaction of load is a sufficient condition for that the OPF problem over a tree network has zero duality gap [34] and the SOCP relaxation is exact [33]. Moreover, it has been shown that the optimal solutions for the problem with the over-satisfaction constraints are expected to make the constraints binding, i.e., the equality will hold for these constraints [35]. In fact, after we solve our problem, we have verified that the equality indeed holds for all these constraints, which means that all the active and reactive powers are balanced.

Problem $\mathcal{P}$ is non-convex because of the non-convex constraints 3, 7 and 16. As to the constraints (3), since the objective of this minimization problem is an increasing function of both the charging and discharging rates, and with the balance constraint (20), these variables are naturally mutual exclusive at the optimal point. Thus we can just remove them because they are incorporated in our formulation implicitly. For the same reason, we can remove constraints (7). In order to tackle the difficulty brought about by constraint (16), we relax it to the following convex inequality constraint:

$$l_{i,t} \geqslant \frac{P_{i,t}^2 + Q_{i,t}^2}{v_{i_0,t}}, \qquad \forall \; t, i \in \mathcal{K} \setminus \{1\}. \tag{24}$$

Using (24), a relaxed problem $\mathcal{P}-relaxed$ is formulated as follows, **Problem $\mathcal{P}-relaxed$**:

$$\min_{X_t} \quad \sum_{t=1}^{H} C_t(X_t)$$

s.t. (2), (4)–(6), (8), (10), (13)–(15), (17) and (20)–(24).

The relaxation is said to be *exact* if (24) is binding at the optimal solution of the problem $\mathcal{P}-relaxed$. The sufficient conditions for the exactness of the relaxation are referred to [21], which have been verified in many real and standard distribution network testbeds. In essence, if the bus voltage is kept around the nominal value and the power injection at each bus is not too large, then the relaxation is exact [16,36]. We assume that these sufficient conditions hold in our problem, and this can be easily proved when the DG penetration level is not too high compared to the load consumption so that there is no reverse power flow. Moreover, we will illustrate the exactness by numerical results (in Section 5). The problem $\mathcal{P}-relaxed$ is then in nature a *second-order cone programming* (SOCP) problem and can be solved by convex optimization solvers such as CVX.

4. Distributed algorithm

We focus on developing a distributed algorithm for solving the problem $\mathcal{P}-relaxed$ in this section, which has many advantages over a centralized method in terms of scalability, privacy, etc. In our approach, each agent (MG or LAO) only needs to communicate with its neighbors and there is no central node. Additionally, the proposed distributed method can be proved to converge to the optimal solution.

Specifically, our problem can be reformulated into a *global variable consensus optimization* (*consensus* for short) problem and be solved based on the ADMM [23]. Thus, we first introduce the ADMM framework and then describe our distributed approach.

4.1. ADMM

The ADMM algorithm solves problems in the form:

minimize $\quad f(x) + g(z)$
subject to $\quad Ax + Bz = c,$ (25)

and its corresponding augmented Lagrangian is:

$$L_\rho(x,y,z) = f(x) + g(z) + y^T(Ax + Bz-c) + (\rho/2)\|Ax + Bz-c\|_2^2. \tag{26}$$

The algorithm consists of the following iterations:

$$x^{k+1} = \underset{x}{\arg\min} \; L_\rho(x,z^k,y^k), \tag{27.1}$$

$$z^{k+1} = \underset{z}{\arg\min} \; L_\rho(x^{k+1},z,y^k), \tag{27.2}$$

$$y^{k+1} = y^k + \rho(Ax^{k+1} + Bz^{k+1}-c), \tag{27.3}$$

where $\rho > 0$. The convergence properties are referred to in [23, §3.2], with quite moderate assumptions (i.e., f and g are closed, proper and convex and L_0 (i.e, Eq. (26) with $\rho = 0$) has a saddle point). Next, we will introduce our ADMM-based distributed algorithm.

4.2. Distributed algorithm for our problem

In our problem, we consider each MG and the LAO as an individual agent. Then, the objective and constraints are separable with respect to this split. Specifically, the first two terms in the objective can be viewed as the cost of the LAO with corresponding constraints (13)–(15), (17) and (21)–(24), then the last two terms in the objective and the remaining constraints can be handled by each MG separately. However, since the distinct $N + 1$ agents share some variables, which make them couple with each other, we make local copies of every coupling variable and assign them to each agent involved, to decouple them. Moreover, we add additional equality constraint to make every copy of the same shared variable equal to the global one, which we call the consensus. This is a generalized consensus problem since each agent involves only some element of the global variable. Therefore, we make copies of those shared variables instead of all of them to reduce the complexity.

In detail, $P_{i_n,t}^A$ is the variable shared by MG_n and the LAO because of constraints (13) and (20), while $T_{m,n,t}$ and $T_{n,m,t}$ are shared by MG_n and MG_m via (20). Therefore, we denote these coupling variables as $X_{cp,t}^{n(l)} = (P_{i_n,t}^{A(mg,l)}, T_{m,n,t}^{(l)}, T_{n,m,t}^{(l)})$, $\forall \; m \neq n$, for the local copies of coupling variables of MG_n, and its consensus counterpart is with superscript c: $X_{cp,t}^{n(c)} = (P_{i_n,t}^{A(c)}, T_{m,n,t}^{(c)}, T_{n,m,t}^{(c)})$. Similarly, we denote the local copies and consensus of the shared variables of the LAO as: $X_{cp,t}^{lao(l)} = (P_{i_n,t}^{A(lao,l)})$ and $X_{cp,t}^{lao(c)} = (P_{i_n,t}^{A(c)})$. Since all the other variables are not shared, they do not need to be copied and have only the consensus, i.e., $X_{nc,t}^{n(c)} = (P_{n,t}^{ESC(c)}, P_{n,t}^{ESD(c)})$ for MG_n and $X_{nc,t}^{lao(c)} = (P_{i,t}^{(c)}, Q_{i,t}^{(c)}, v_{i,t}^{(c)}, l_{i,t}^{(c)}, P_{i,t}^{A(c)}, Q_{i,t}^{A(c)})$ for the LAO. Furthermore, we use some symbols to denote the different constraint sets for simplicity. We denote Ω_n^l as the set of variables that satisfy constraint (20), for each MG_n, and Ω_{lao}^l as the set of variables satisfying constraint (13). In addition, we denote Ω_n^c as the set of those satisfying constraints (2), (4)–(6), (8) and (10), while Ω_{lao}^c denotes the set of those satisfying constraints Eqs. (14), (15), (17), (23), and (24). As to the objective function, we use $C_{lao,t}(X_t^{lao})$ to denote the first two terms in $C_t(X_t)$, and $C_{n,t}(X_t^n) = \omega_3 C_{n,t}^{ES} + \frac{1}{2}\omega_4 \sum_{(v,w) \in \Theta_n} \frac{r_{v,w} T_{v,w,t}^2}{U_{v,w}^2}$ to denote the split of the last two terms in terms of each MG_n, where $\Theta_n = \{(v,w)|v,w \in \mathcal{W}, v = n \text{ or } w = n \text{ but } v \neq w\}$. In this way we can transform the problem $\mathcal{P}-relaxed$ as follows:

$$\min \ \sum_{t=1}^{H} (C_{lao,t}(X_t^{lao}) + \sum_{n \in \mathscr{W}} C_{n,t}(X_t^{n})) \tag{28}$$

$$\text{s.t.} \quad X_{cp,t}^{n(l)} \in \Omega_n^l, \quad X_{np,t}^{n(c)} \in \Omega_n^c, \tag{29}$$

$$X_{cp,t}^{lao(l)} \in \Omega_{lao}^l, \quad X_{np,t}^{lao(c)} \in \Omega_{lao}^c, \tag{30}$$

$$X_{cp,t}^{lao(l)} = X_{cp,t}^{lao(c)}, \quad X_{cp,t}^{n(l)} = X_{cp,t}^{n(c)}. \tag{31}$$

Now, the formulation above has the same form as (25) so the ADMM based algorithm (i.e., Eqs. (27.1)–(27.3)) can be applied, which are known as *x-update*, *z-update* and *dual variable update* steps, respectively. For *x-update*, since the objective and constraints are separable in terms of agents, this update can be conducted in parallel and in a distributed manner. Specifically, at the *(k + 1)-th* step, the LAO's *x-update* solves

$$\min \ \sum_{t=1}^{H} C_{lao,t}(X_t^{lao}) + (y_{lao}^{(k)})^T X_{cp,t}^{lao(l)} + \rho/2\|X_{cp,t}^{lao(l)} - X_{cp,t}^{lao(c)(k)}\|_2^2$$
$$\text{s.t.} \quad (30), \tag{32}$$

and the MG_n's *x-update* solves

$$\min \ \sum_{t=1}^{H} C_{n,t}(X_t^{n}) + (y_n^{(k)})^T X_{cp,t}^{n(l)} + \rho/2\|X_{cp,t}^{n(l)} - X_{cp,t}^{n(c)(k)}\|_2^2$$
$$\text{s.t.} \quad (29), \tag{33}$$

where $y_{lao}^{(k)}$ and $y_n^{(k)}$ are dual variables of the LAO and MG_n, respectively. The *z-update* step takes the average of the shared variables' copies and assigns it to the consensus variables at the *(k + 1)-th* step (as shown in [23]). In the *dual variable update* step, the dual variables are separately updated to drive the variables into the consensus, given by (33 and 34), for the LAO and MG_n, respectively:

$$y_{lao}^{(k+1)} = y_{lao}^{(k)} + \rho(X_{cp,t}^{lao(l)(k+1)} - X_{cp,t}^{lao(c)(k+1)}), \tag{34}$$

$$y_n^{(k+1)} = y_n^{(k)} + \rho(X_{cp,t}^{n(l)(k+1)} - X_{cp,t}^{n(c)(k+1)}). \tag{35}$$

Note that in general, the *z-update* needs to be handled by a central collector. However, in our problem, the coupling variables $P_{in,t}^A$ and $T_{m,n,t}$ are shared solely between 2 neighbors (i.e., MG_n & LAO, MG_m & MG_n, respectively), which means that the *z-update* step (averaging step) can be done by communications among neighbors and, consequently, no central collector is needed. Then, the *z-update* is carried out in a fully distributed fashion. To sum up the aforementioned steps, we

Algorithm 1. ADMM-based fully distributed algorithm

1: **Initialization:** $k \leftarrow 0$, all the dual variables $y_n^{l(0)}$, $y_{lao}^{l(0)}$ and primal variables $X_{cp,t}^{n(l)(0)}$, $X_{np,t}^{n(c)(0)}$, $X_{cp,t}^{n(c)(0)}$ $X_{cp,t}^{lao(l)(0)}$, $X_{np,t}^{lao(c)(0)}$, $X_{cp,t}^{lao(c)(0)}$ are initialized to 0, $k \leftarrow 1$, **input** ρ.

2: **Repeat:**

3: *x-update* in parallel: the LAO solves (32) and MG_n solves (33) to get the *(k + 1)-th* values.

4: *z-update* in parallel: each agent communicates with its neighbors and takes an average on the shared variables' copies to get the *(k + 1)-th* consensus.

5: *dual variable update* in parallel: the LAO updates by (34) and MG_n does it by (35).

6: $k \leftarrow k + 1$

7: **Until:** convergence conditions are satisfied (the primal and dual residuals are small) [23, §3.3.1].

propose the method in Algorithm 1 and the convergence of this proposed method is assured by the following theorem.

Theorem 1. *The solution of the proposed ADMM-based distributed algorithm can converge to the optimal solution of problem $\mathscr{P}$−relaxed.*

Proof. First, we combine constraint (31) to a compact form $AX_t^{(l)} = X_t^{(c)}$, where $X_t^{(c)}$ and $X_t^{(l)}$ represent local copies and the consensus of the shared variables, respectively. Then, the reformulated problem (28) is a two block consensus problem as described in [37]. Thus, the sufficient conditions for the ADMM to converge to the optimal solution under convexity of the objective function and constraint sets is that the matrix A has full column-rank [37]. Due to the fact that each of the coupling variables are shared only between the two direct neighbors in our problem, A can be easily derived and shown to satisfy this condition. □

It should be noted that the convergence result of our proposed ADMM-based algorithm is stronger than a general convergence result of the ADMM algorithm applied to a convex problem, where the primal variables need not converge to the optimal values [23, §3.2.1]. Furthermore, in Algorithm 1, at each iteration, MGs and the LAO only need to update the local copies of the shared variables, and then communicate with neighbors to update the consensus, followed by the dual variable update, and so forth. Finally, different copies are driven to be identical to the mutual consensus. Since every update can be taken in parallel among agents, this algorithm is distributed.

5. Numerical results

5.1. A 34-bus radial distribution network

We apply our energy management model on a 34-bus radial distribution network, as shown in Fig. 4. It is noted that in this figure, while each MG is represented by a circle and connected to the distribution network via a point of common coupling, it does not mean that a MG only has one node. In fact, a MG can include several nodes of the network inside of it and in this paper, we mainly focus on the co-operation and interaction among MGs and the main grid. Therefore, the topology inside a MG is not shown here. This radial network has a main feeder and 4 laterals with a rated voltage of 22 kV and an allowed voltage range of ±5%. Details and load data can be found in [38] with some slight modifications. We assume that three MGs ($N = 3$) are located at nodes 4, 8, and 19, respectively. All the other nodes are pure loads (for $i \in \{2,3...34\} \backslash \{4,8,19\}$, $K = 34$) except node 1, which is a slack bus. For the EEN, we consider 4 different topologies as in Fig. 5, and the

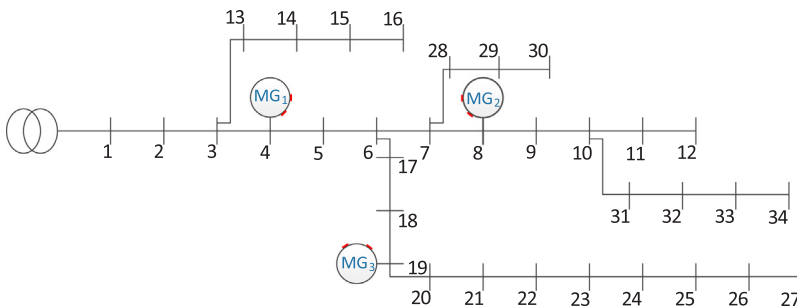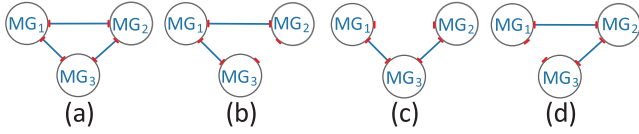**Fig. 4.** A 34-bus radial distribution network.

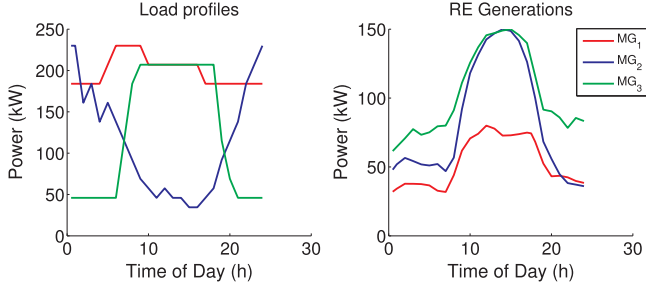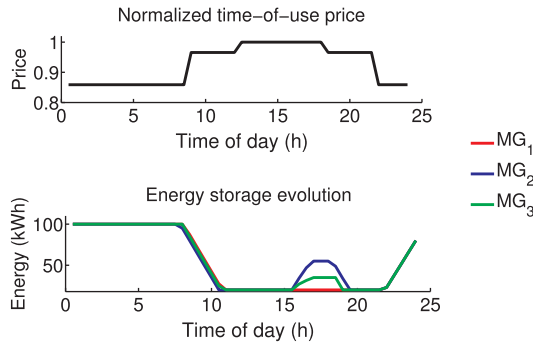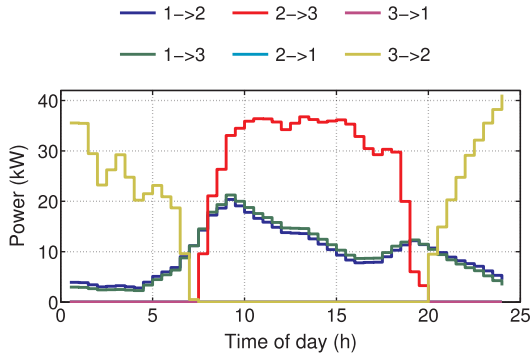**Fig. 5.** Four different EEN topologies.

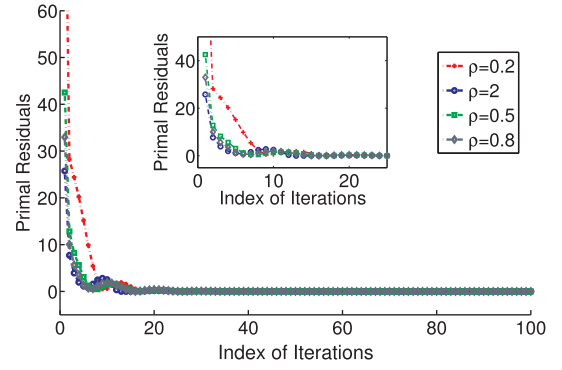**Fig. 6.** Load and renewable energy generation profiles.
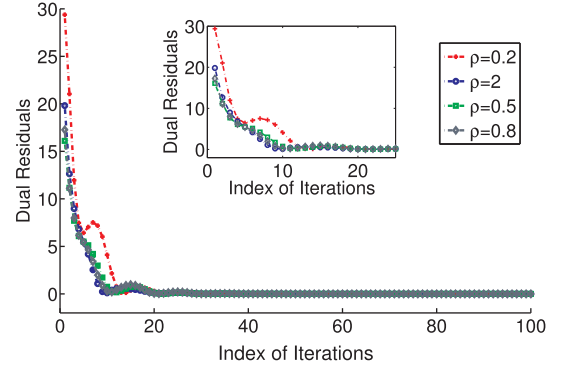

(a) TOU price and DS evolutions.

(b) Energy transmission in EEN.

Fig. 7. Normalized price, energy storage evolutions and power transmissions in EEN.
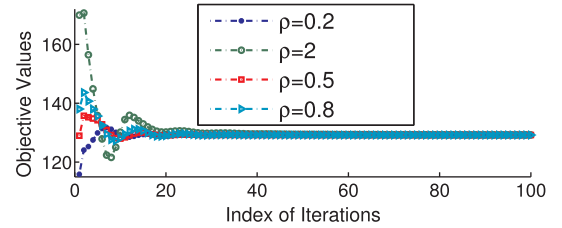

(a) Primal residuals.

(b) Dual residuals.

Fig. 8. Evolutions of primal & dual residuals for different values of ρ.

Fig. 9. Evolutions of objective values for different ρ.

Table 1
Loss comparison for different topologies.

Cases	$loss_1$ (10^6)	$loss_2$ (10^4)	$loss_3$ (10^4)
w/o EEN	1.0820	2.4542	0
Case (a)	1.0710 (1.02%)	2.4214 (1.34%)	1.2716
Case (b)	1.0722 (0.91%)	2.4457 (0.35%)	1.1541
Case (c)	1.0757 (0.58%)	2.4325 (0.89%)	0.7185
Case (d)	1.0760 (0.56%)	2.4263 (1.14%)	0.6929
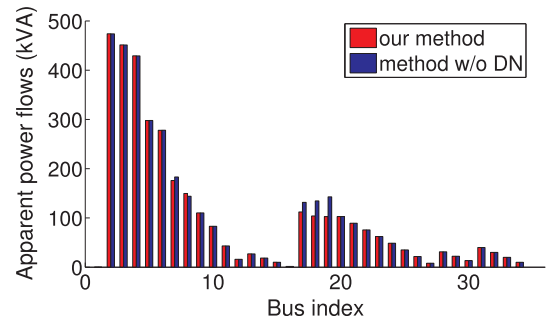
Fig. 10. Maximum power flow over buses (34-bus testbed).

line resistances ($MG_1 \leftrightarrow MG_2$, $MG_1 \leftrightarrow MG_3$, $MG_2 \leftrightarrow MG_3$) are 2.5 Ω, 2.5 Ω and 0.075 Ω, respectively. The transmission voltage $U_{i,j} = 1.58$ kV, $\forall~i,j \in \{1,2,3\}, i \neq j$. Time is slotted into 48 intervals for 24 h ($H = 48$), so $\Delta = 0.5$ h. $\overline{ES_n} = 100$ kWh and $\underline{ES_n} = 0.2\overline{ES_n}$ for each MG. The charging and discharging efficiencies are $\eta_c = 0.95$ and $\eta_d = 1$, respectively. Furthermore, $\underline{\gamma_n} = 0.8$, and $\overline{\gamma_n} = 1$. The charging and discharging rates limit is 30 kW and the weighting factors $\{\omega_i, i = \{1,2,3,4\}\}$ are $\{0.1,5,0.3,2\}$. The load profiles for different buses are some typical consumption profiles from Slovenian distribution companies [39] and the TOU price is the *Summer Rate* obtained from the website of *PG & E Company* [40], shown in Figs. 6 and 7a, respectively. The renewable energy generation profiles are from *California Independent System Operator* [41] and the generation capacities are 80 kW, 150 kW and 150 kW for MG_n, $n \in \{1,2,3\}$, respectively.
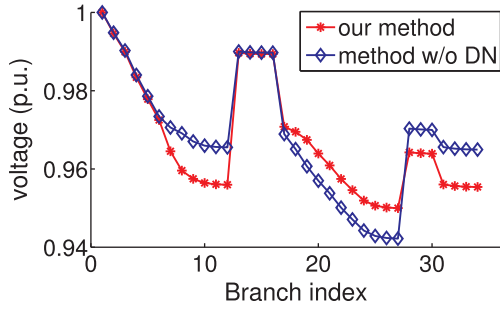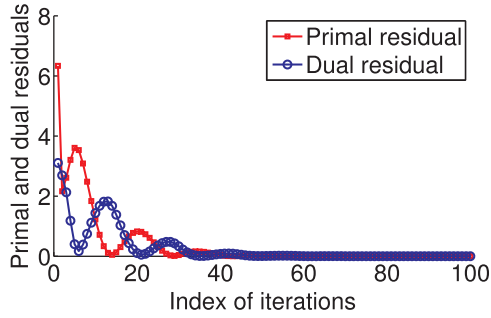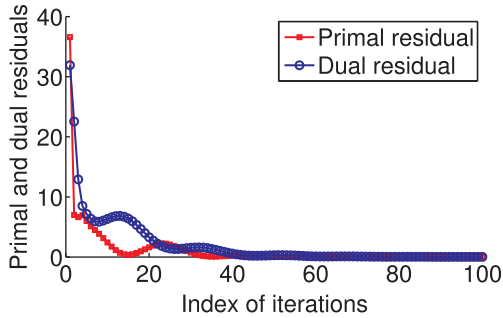
Fig. 11. Minimum voltage over buses (34-bus testbed).

(a) A 69-bus test system.

(b) A 119-bus test system.

Fig. 12. Primal and dual residuals for two testbeds.

From Fig. 6, we can see that different MGs have different consumption profiles during the day and night. More specifically, MG_1 behaves as an industrial user who has a continuous high demand during the day. MG_2 is a typical residential user with low power consumption during working hours while the peak demand appears during the night. In contrast, MG_3 shows complementary behavior to MG_2, which is common for commercial users. Their renewable energy generation profiles are similar, in view of that they are not too far away from each other and correlations are assumed to exist among MGs.

With the numerical results, we have verified that constraint (24) is indeed binding at the optimal solution of problem $\mathscr{P}-relaxed$, which

shows that the solution is also optimal for original problem $\mathscr{P}$. Then we demonstrate the optimal energy management strategies in terms of DS units and MG energy exchange for the fully connected EEN topology (case (a)) in Fig. 5. First, in Fig. 7a, on the one hand, all MGs choose to discharge at around 9 a.m. when the electricity price starts to rise, which reduces energy purchase from the main grid. On the other hand, they recharge at midnight when the price is the lowest. Second, Fig. 7b gives the detailed energy transmissions in the EEN. It can be seen that MG_1 always transmits energy to the other two MGs because MG_1 is closer to the feeding entry (*Bus 1*) of the distribution network, and a mass of power flows by MG_1 to feed the downstream part of the distribution network. Therefore, it is reasonable to transmit energy by *short path* from MG_1 to the other two MGs. However, the inverse transmission is not preferable because it is opposite to the main power flow direction. Another result is that the energy transmission between MG_2 and MG_3 changes directions alternately. We can see that during the morning (from 00:00 to 06:00) and night (from 20:00 to 24:00) periods, MG_3 has an energy surplus while MG_2 has an energy deficiency. In this case, MG_3 acts as a supplier during this period while it becomes a receiver during working hours. In summary, Fig. 7b demonstrates the dynamic interaction among MGs according to their distinct energy consumption behaviors and relative geographical locations in the distribution network.

Figs. 8 and 9 show the convergence performance of Algorithm 1 against different parameters ρ, ranging from 0.2 to 2. It can be seen that different choices of ρ can make a difference at the beginning of the algorithm, and after several dozens of iterations, all of them can converge. The same phenomena can be observed for the evolution of objective values. Therefore, our algorithm has good performance in convergence rate and is not too sensitive to the value of ρ, except for the first several iterations.

Table 1 lists the comparisons of different losses among different EEN topologies. In the table, $loss_n$, $n \in \{1,2,3\}$, represent the loss of power flow, the battery's conversion loss and the MG energy exchange loss, respectively. The four EEN topologies are compared with the one without direct energy exchange, and their improvements (i.e., the reduced loss in %) are shown in parentheses. From the table, it is clear that the fully connected topology, case (a), can bring the highest reductions of $loss_1$ & $loss_2$. While for the other three cases, case (b) has advantages over the other two, since it improves the most for $loss_1$, which achieves the largest loss reduction, although it has a worse performance in terms of $loss_2$ & $loss_3$, which have a much lower order of magnitude compared to $loss_1$. Consistent with the previous results (Fig. 7b), the transmission lines between MG_1 and the other two MGs play the most important role and this can give us some insight into which links are the most beneficial links for a specific geographical location in the MGs network. For the planning of the EEN, the comparison among different topologies helps balance the trade-off between the capital cost of EEN constructions and the benefit that EEN can bring.

In addition, to demonstrate that our methods can successfully manage the energy of microgrids while ensuring that the voltage and power flow limits are not violated, we make a comparison of our results
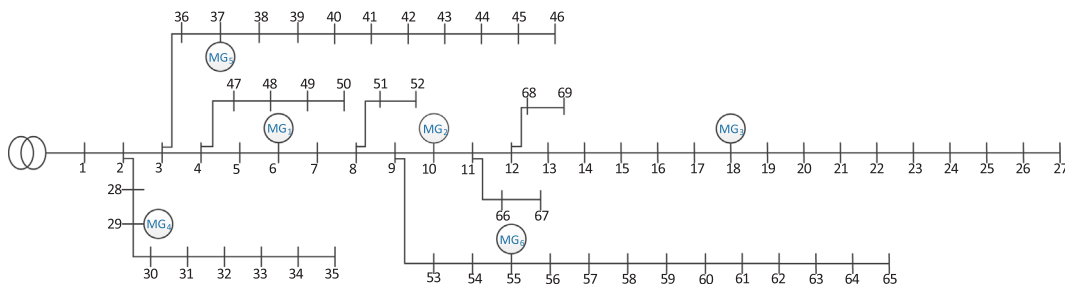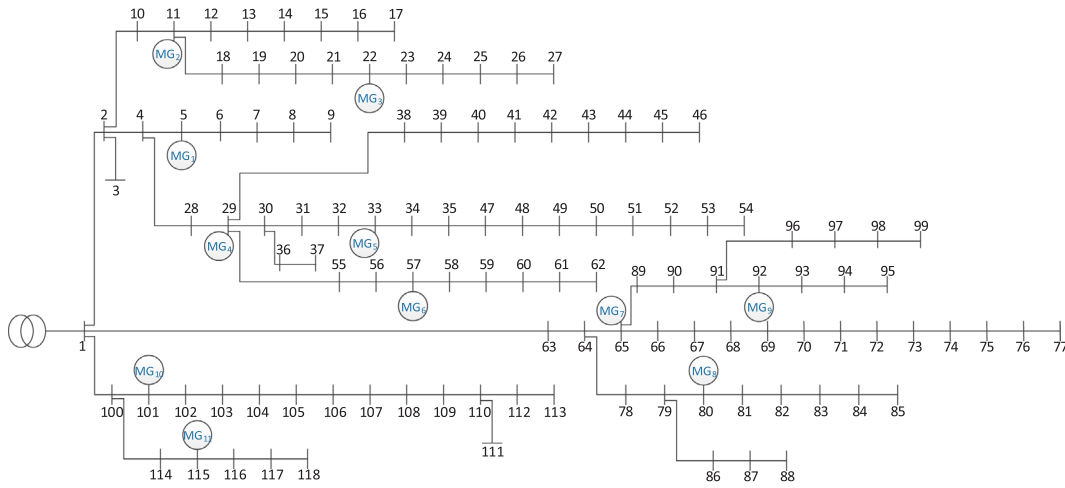

Fig. 13. A 69-bus test system.

Fig. 14. A 119-bus test system.

Table 2
Relative errors (%) of the MPC-based approach without prediction error.

$\overline{ES_n}$ (kWh)		100		200	
$\overline{P_{n,t}^{ESC}}$ (kW)		30	10	30	10
W (h)	1	0.93	0.55	1.13	0.57
	2	0.35	0.24	0.59	0.41
	3	0.31	0.22	0.23	0.38
	4	0.71	0.35	0.80	0.49
	5	1.10	0.42	1.18	0.50
	6	0.44	0.25	0.68	0.40
	7	0.34	0.23	0.60	0.34
	8	0.35	0.21	0.56	0.31

Table 3
Relative errors (%) of the MPC-based approach with prediction errors.

$\overline{ES_n}$ (kWh)		100		200	
$\overline{P_{n,t}^{ESC}}$ (kW)		30	10	30	10
W (h)	1	0.93	0.55	1.13	0.57
	2	0.35	0.24	0.59	0.41
	3	0.31	0.22	0.51	0.38
	4	0.72	0.34	0.95	0.49
	5	1.10	0.41	1.29	0.50
	6	0.45	0.25	0.64	0.40
	7	0.35	0.22	0.57	0.34
	8	0.35	0.21	0.55	0.31

with those which ignore the underlying distribution network. For the 34-bus testbed distribution network, the minimum voltage profiles and the maximum apparent power flows over the time horizon are shown in Figs. 10 and 11. In Fig. 10, we can see that if the underlying distribution network is ignored, the power flows on some branches can be, from 4% (*bus 5*) to 39% (*bus 19*), higher than those of our method. Moreover, in Fig. 11, it can be seen that some bus voltages (*bus 23* to *bus 27*) are lower than the stable voltage limit (which is 0.95 p.u. in our simulation). Therefore, from Figs. 10 and 11, we can see that if the energy management problems are carried out without considering the underlying distribution network like the existing methods in the literature, the voltage limits and power flow limits may be violated, which will damage the security and stability of the system. By contrast, our method successfully manages the energy of microgrids without violating any system operational constraint by taking the distribution network into account.

5.2. 69-bus and 119-bus test systems

In order to show the scalability of our method for larger systems, we have performed more simulations on a 69-bus distribution network [42] with 6 microgrids (Fig. 13) and a 119-bus distribution network test system [43] with 11 microgrids (Fig. 14), where $\rho = 1$ for all the simulations. Our proposed ADMM algorithm is solved by the CVX solver on a single machine with an i5 dual-core processor, while the computations for each agent are carried out in a parallel way with the help of the Parallel Computing Toolbox in MATLAB. The convergence of primal and dual residuals for these two test systems are shown in Fig. 12. From the figure, we can see that, for larger systems, our algorithm also has good performance in the convergence rate. Specifically, it only takes several dozens of iterations to converge, which is similar to the case of the 34-bus system. Therefore, our proposed distributed algorithm is scalable and applicable to large systems. From the simulation results in Figs. 8, 9 and 12, the good convergence performance of our method is demonstrated and thus, the communication burden with this small number of iterations is tractable. Furthermore, since our algorithm is carried out in a distributed manner, at each iteration the agent only needs to update the information with its direct neighbors and this will alleviate the communication burden. Additionally, considering that the ADMM algorithm has been widely employed in lots of applications, many acceleration techniques [44,45] have been studied based on the ADMM method to further improve the convergence performance. For example, in [44,45], a restarting rule is applied based on the ADMM algorithm and a faster convergence performance has been observed in a variety of problems. Therefore, even though our algorithm has shown a good convergence performance, it can be beneficial to leverage various accelerating techniques such that our ADMM-based distributed algorithm can be further improved.

5.3. Implementation with an MPC-based approach

In the simulations above, we assume that a perfect estimation of the input of renewable energy to facilitate the operations of our proposed scheme since we are focusing on the day-ahead market. To render our proposed method more realistic, we have integrated it into the framework of MPC-based approach to solve the problem. Compared to the on-line ADMM method proposed in [29] for solving the energy management problem of networked MGs, the MPC-based approach can exploit the prediction information of the renewable energy generation for several hours in advance, which is not taken into account in the on-line ADMM algorithm. Specifically, we assume that there is a window with the size of *W* hours, which means that we can have a prediction (either with or without errors) of the energy price, the renewable energy

generation outputs and the loads for the future W hours. Therefore, at each time slot t_α, we solve the energy management problem from t_α to $t_\alpha + W$ as follows,

$$\min_{X_t} \sum_{t=t_\alpha}^{t_\alpha + W} C_t(X_t) \tag{36}$$

s.t. all the constraints, $\forall\, t \in [t_\alpha, t_\alpha + W]$.

After the problem is solved, only the optimal decision at the first step $t = t_\alpha$ is applied. Then the window moves to the next time slot $[t_\alpha + 1, t_\alpha + 1 + W]$ with the updated prediction information. This procedure is repeated until the end of the entire time horizon $(t_\alpha + W = H)$. The implementation of integrating our algorithm into the MPC-based approach is as follows:

(1) Given a window size W, at $t_\alpha = 1$, initialize the prediction of the energy price, the renewable generation outputs and the loads for $t \in [t_\alpha, t_\alpha + W]$.
(2) Solve Problem (36) for $t \in [t_\alpha, t_\alpha + W]$ and carry out the optimal decision at the first time slot t_α.
(3) If $t_\alpha + W < H$, then $t_\alpha \leftarrow t_\alpha + 1$ and update the prediction information. Go back to Step (2) and repeat the procedure until the end of the time horizon.

When we implement our algorithm with the MPC-based approach, two kinds of case studies are carried out depending on whether the prediction errors within the prediction windows are taken into account. In the first case, we assume that a perfect prediction can be obtained for the energy price, the renewable energy generation outputs and the loads within the window of future W hours. In the second case, we consider that at time $t = t_\alpha$, the renewable generation data at the current time slot $t = t_\alpha$ can be known perfectly, while there is an additional noise applied to the predicted renewable generation data for the future time slots in the window $t \in [t_\alpha + 1, t_\alpha + W]$. The noise for the renewable energy outputs of MG_n at each time slot is assumed to follow a normal distribution $N(0, \sigma_n)$, where σ_n denotes the standard deviation of the error distribution. In our case studies, we set: $\sigma_1 = 2.5\,\text{kW}$, $\sigma_2 = 5\,\text{kW}$ and $\sigma_3 = 5\,\text{kW}$, respectively.

Next, for both cases with and without prediction errors of the renewable energy generation, we compare the objective value obtained from our proposed method implemented with an MPC-based approach for different window sizes (W), i.e., $W = 1,2,...,8$ hours, with the real optimal objective value which is obtained by assuming that the renewable generation is perfectly predicted for the whole time horizon. The simulations are carried out for different scenarios with different energy storage capacities ($\overline{ES_n}$), i.e., $\overline{ES_n} = 100\,\text{kWh}$, or $200\,\text{kWh}$, $n = 1,2,3$, and different charging and discharging power limits, i.e., $\overline{P_{n,t}^{ESC}} = \overline{P_{n,t}^{ESD}} = 30\,\text{kW}$, or $10\,\text{kW}$, $n = 1,2,3$. The relative errors (ϵ) of the objective values obtained by the MPC-based approach and the real one are shown in Tables 2 and 3 corresponding to the cases without and with prediction errors, respectively.

From the tables, it can be seen that, for both cases, the relative performance loss of applying our method with an MPC-based approach are quite small. Particularly, when the charging and discharging power limits are small, the MPC-based method works very well. This is because at each time slot, very aggressive charging/discharging actions are avoided to ensure that there is enough storage buffer for the future use. In addition, the performance of the two cases is very close to each other. This is because only the decision at the first time slot of each window is implemented, and thus the small prediction errors will not incur much performance loss under the MPC-based approach. Therefore, it is validated that by implementing our method with the MPC-based approach, the performance loss due to the prediction errors is acceptable.

6. Conclusions

In this work, we studied the energy management problem for co-operative MGs with direct energy exchange under the distribution network and developed a distributed algorithm. We formulated the energy management problem as a practical yet non-convex optimization problem to minimize the total system cost. After exploiting an exact relaxation of the non-convex constraint, we equivalently transformed this problem into an *SOCP* problem and thus made it efficiently solvable. Then convergence of our ADMM-based method was proved and verified with numerical results. By applying our model to three distribution network testbeds, we showed the scalability of our proposed method and also, we found a cooperation between energy storage devices and the EEN among heterogeneous MGs, instead of solely relying on the main grid to satisfy their load demands. Another finding was that the MG that was closer to the upstream part of the distribution network had a tendency to act as an energy supplier in the EEN, which could bring a lower cost. What's more, the performances of different EEN topologies were tested and we found that certain transmission lines were more beneficial than others.

This work can be further extended in two directions. First, we will take into account the intermittency of renewable generation and demand, for which the current deterministic methods would be no longer applicable. Second, we will investigate the detailed internal trading mechanism, such as how to control the pricing in the EEN to encourage energy sharing among different MGs.

Acknowledgment

References

[1] Katiraei F, Iravani R, Hatziargyriou N, Dimeas A. Microgrids management. IEEE Power Energy Magaz 2008;6(3):54–65.
[2] Giotitsas C, Pazaitis A, Kostakis V. A peer-to-peer approach to energy production. Technol Soc 2015;42:28–38.
[3] Wu Y, Tan X, Qian L, Tsang DHK, Song W-Z, Yu L. Optimal pricing and energy scheduling for hybrid energy trading market in future smart grid. IEEE Trans Indust Inf 2015;11(6):1585–96.
[4] Qian LP, Zhang YJA, Huang J, Wu Y. Demand response management via real-time electricity price control in smart grids. IEEE J Select Areas Commun 2013;31(7):1268–80.
[5] Gregoratti D, Matamoros J. Distributed energy trading: the multiple-microgrid case. IEEE Trans Indust Electron 2015;62(4):2551–9.
[6] Werth A, Kitamura N, Tanaka K. Conceptual study for open energy systems: distributed energy network using interconnected dc nanogrids. IEEE Trans Smart Grid 2015;6(4):1621–30.
[7] Werth A, Andre A, Kawamoto D, Morita T, Tajima S, Yanagidaira D, et al. Peer-to-peer control system for dc microgrids. IEEE Trans Smart Grid, doi:http://dx.doi.org/10.1109/TSG.2016.2638462 [in press].
[8] Lakshminarayana S, Quek TQ, Poor HV. Cooperation and storage tradeoffs in power grids with renewable energy resources. IEEE J Select Areas Commun 2014;32(7):1386–97.
[9] Ouammi A, Dagdougui H, Dessaint L, Sacile R. Coordinated model predictive-based power flows control in a cooperative network of smart microgrids. IEEE Trans Smart Grid 2015;6(5):2233–44.
[10] Fathi M, Bevrani H. Statistical cooperative power dispatching in interconnected microgrids. IEEE Trans Sustain Energy 2013;4(3):586–93.
[11] Mondal A, Misra S, Obaidat MS. Distributed home energy management system with storage in smart grid using game theory. IEEE Syst J 2015(99).
[12] Zhu T, Huang Z, Sharma A, Su J, Irwin D, Mishra A, et al. Sharing renewable energy in smart microgrids. In: Proceedings of the ACM/IEEE 4th international conference on cyber-physical systems; 2013. p. 219–28.
[13] Hong Y, Goel S, Liu WM. An efficient and privacy-preserving scheme for p2p energy exchange among smart microgrids. Int J Energy Res 2016;40(3):313–31.
[14] K. Rahbar, C.C. Chai, R. Zhang, Real-time energy management for cooperative microgrids with renewable energy integration, in: 2014 IEEE International Conference on Smart Grid Communications (SmartGridComm), 2014, pp. 25–30.
[15] C. Wei, Z.M. Fadlullah, N. Kato, I. Stojmenovic, A novel distributed algorithm for power loss minimizing in smart grid, in: 2014 IEEE International Conference on Smart Grid Communications (SmartGridComm), 2014, pp. 290–295.
[16] Shi W, Li N, Xie X, Chu C-C, Gadh R. Optimal residential demand response in

distribution networks. IEEE J Select Areas Commun 2014;32(7):1441–50.

[17] Wang Z, Chen B, Wang J, Begovic MM, Chen C. Coordinated energy management of networked microgrids in distribution systems. IEEE Trans Smart Grid 2015;6(1):45–53.

[18] Tan S, Xu J-X, Panda SK. Optimization of distribution network incorporating distributed generators: an integrated approach. IEEE Trans Power Syst 2013;28(3):2421–32.

[19] Majumder R. Some new aspects of stability in microgrids. IEEE Trans Power Syst 2013;28(3):3243–52.

[20] Liu T, Tan X, Sun B, Wu Y, Guan X, Tsang DHK. Energy management of cooperative microgrids with p2p energy sharing in distribution networks. In: 2015 IEEE international conference on smart grid communications (SmartGridComm); 2015. p. 410–5.

[21] Low SH. Convex relaxation of optimal power flow-part i: formulations and equivalence. IEEE Trans Control Netw Syst 2014;1(1):15–27.

[22] Dall'Anese E, Zhu H, Giannakis GB. Distributed optimal power flow for smart microgrids. IEEE Trans Smart Grid 2013;4(3):1464–75.

[23] Boyd S, Parikh N, Chu E, Peleato B, Eckstein J. Distributed optimization and statistical learning via the alternating direction method of multipliers. Found Trends® Mach Learn 2011;3(1):1–122.

[24] Wang Z, Chen B, Wang J, et al. Decentralized energy management system for networked microgrids in grid-connected and islanded modes. IEEE Trans Smart Grid 2016;7(2):1097–105.

[25] Lv T, Ai Q, Zhao Y. A bi-level multi-objective optimal operation of grid-connected microgrids. Electr Power Syst Res 2016;131:60–70.

[26] Lv T, Ai Q. Interactive energy management of networked microgrids-based active distribution system considering large-scale integration of renewable energy resources. Appl Energy 2016;163:408–22.

[27] Lu T, Wang Z, Ai Q, Lee W-J. Interactive model for energy management of clustered microgrids. IEEE Trans Indust Appl 2017;53(3):1739–50.

[28] Kim B, Bae S, Kim H. Optimal energy scheduling and transaction mechanism for multiple microgrids. Energies 2017;10(4):566.

[29] Ma W-J, Wang J, Gupta V, Chen C. Distributed energy management for networked microgrids using online alternating direction method of multipliers with regret. IEEE Trans Smart Grid, doi:http://dx.doi.org/10.1109/TSG.2016.2569604 [in press].

[30] Tan X, Wu Y, Tsang DH. Pareto optimal operation of distributed battery energy storage systems for energy arbitrage under dynamic pricing. IEEE Trans Paral

[31] Tan X, Wu Y, Tsang DH. A stochastic shortest path framework for quantifying the value and lifetime of battery energy storage under dynamic pricing. IEEE Trans Smart Grid 2017;8(2):769–78.

[32] Baran ME, Wu FF. Network reconfiguration in distribution systems for loss reduction and load balancing. IEEE Trans Power Deliv 1989;4(2):1401–7.

[33] Farivar M, Low SH. Branch flow model: relaxations and convexification (part I). IEEE Trans Power Syst 2013;28(3):2554–64.

[34] Bose S, Gayme DF, Low S, Chandy KM. Optimal power flow over tree networks. In: 2011 49th Annual Allerton conference on communication, control, and computing (Allerton); 2011. p. 1342–8.

[35] Lavaei J, Low SH. Zero duality gap in optimal power flow problem. IEEE Trans Power Syst 2012;27(1):92–107.

[36] Peng Q, Low SH. Distributed algorithm for optimal power flow on a radial network. In: 53rd IEEE conference on decision and control; 2014. p. 167–72.

[37] Mota JF, Xavier JM, Aguiar PM, Püschel M. D-admm: a communication-efficient distributed algorithm for separable optimization. IEEE Trans Sig Process 2013;61(10):2718–23.

[38] Chis M, Salama M, Jayaram S. Capacitor placement in distribution systems using heuristic search strategies. IEE Proc-Gener, Transm Distrib 1997;144(3):225–30.

[39] Gerbec D, Gasperic S, Smon , Gubina F. Consumers' load profile determination based on different classification methods. In: IEEE power engineering society general meeting, vol. 2; 2003.

[40] PG & E. Summer time-of-use rates < http://www.pge.com/en/mybusiness/rates/tvp/toupricing.page?WT.mc_id=Vanity_touintro > [accessed: 2010-09-30].

[41] California ISO. Daily renewables output data for 04/11/2015, 03/31/2015 and 09/25/2015 < http://www.caiso.com/market/Pages/ReportsBulletins/DailyRenewablesWatch.aspx > [accessed: 2010-09-30].

[42] Baran ME, Wu FF. Optimal capacitor placement on radial distribution systems. IEEE Trans Power Deliv 1989;4(1):725–34.

[43] Zhang D, Fu Z, Zhang L. An improved ts algorithm for loss-minimum reconfiguration in large-scale distribution systems. Electr Power Syst Res 2007;77(5):685–94.

[44] Kadkhodaie M, Christakopoulou K, Sanjabi M, Banerjee A. Accelerated alternating direction method of multipliers. In: Proceedings of the 21th ACM SIGKDD international conference on knowledge discovery and data mining; 2015. p. 497–506.

[45] Goldstein T, O'Donoghue B, Setzer S, Baraniuk R. Fast alternating direction optimization methods. SIAM J Imag Sci 2014;7(3):1588–623.